Probing Scotogenic Effects in Higgs Boson Decays

Shu-Yu Ho and Jusak Tandean

Department of Physics and Center for Theoretical Sciences,
National Taiwan University,
Taipei 106, Taiwan

Abstract

The recent observation of a Higgs boson at the LHC and experimental confirmation of the nonvanishing neutrino-mixing parameter $\sin\theta_{13}$ offer important means to test physics beyond the standard model. We explore this within the context of the scotogenic model, in which neutrinos acquire mass radiatively via one-loop interactions with dark matter. Starting with a two-parameter neutrino-mixing matrix which is consistent with the latest neutrino-oscillation data at the one-sigma level, we derive different sets of solutions for the Yukawa couplings of the nonstandard particles in the model and use the results to consider the Higgs decays into final states involving the new particles. Assuming that the lightest one of them serves as fermionic cold dark matter, we show that such decays are allowed by various experimental and theoretical constraints to have substantial rates that are already restricted by the current LHC data. We also look at their correlations with the Higgs decays into $\gamma\gamma$ and γZ. Upcoming LHC measurements of the Higgs boson can therefore either detect scotogenic signals or place further constraints on the model.

I. INTRODUCTION

The recent discovery of a Higgs boson with mass in the 125-126 GeV range at the LHC [1] and experimental confirmation of the neutrino-mixing parameter $\sin\theta_{13}$ that is nonnegligible [2] undoubtedly have far-reaching implications for efforts to identify the nature of physics beyond the standard model (SM). Any realistic scenario for new physics would need to incorporate such a particle and account for neutrino masses and mixing angles of the right amount. In addition, since about 22% of the total cosmic energy density has been inferred from astronomical observations to be attributable to matter that is nonluminous and nonabsorbing [3], the desired new-physics model should also possess at least one candidate for dark matter (DM).

Among the simplest possibilities accommodating the necessary ingredients is the scotogenic model proposed by Ma [4], in which neutrinos get mass radiatively via their one-loop interactions with new particles comprising scalars and fermions, at least one of which plays the role of DM. Here we explore some implications of the aforementioned experimental findings within the context of the minimal version of this model. In particular, identifying the newly observed Higgs boson with the Higgs boson in the model, hereafter denoted by h, and assuming the lightest one of the new fermions to be the DM, we consider the decays of h into final states containing the nonstandard particles in the model. Moreover, since their Yukawa couplings depend on the neutrino-mixing angles and contribute to the decay amplitudes, it is important to adopt parametrization for the couplings that takes into account the fact that $\sin\theta_{13}$ is not negligibly small. Subsequently, we will demonstrate that such exotic decays of h are allowed by various experimental and theoretical constraints to have substantial rates that are already bounded by the existing LHC data. As upcoming measurements at the LHC will pin down the various properties of h with increasing precision, the acquired data will then either reveal hints of the new particles or probe the model more stringently.

The organization of the paper is as follows. The next section gives a description of the relevant Lagrangians and the neutrino mass formula. In Section III, we write down a neutrino-mixing matrix that depends on only two parameters and is consistent with the neutrino-oscillation data, including the measured nonzero θ_{13}, at the one-sigma level. From the resulting neutrino-mass matrix, we derive solutions for the Yukawa couplings of the new particles in the model. In Section IV, we look at a number of experimental and theoretical constraints on their couplings and masses. Specifically, there are low-energy measurements that can limit the Yukawa couplings. Furthermore, the Yukawa couplings belonging to the DM candidate also have to be compatible with the observed relic abundance. In Section V, with the parameter values satisfying the preceding constraints, we investigate the Higgs decays into final states involving the nonstandard particles and take into account extra constraints from the latest LHC data, including those on the Higgs decays into $\gamma\gamma$ and γZ. We also examine the scotogenic impact on the correlations between these different decays. We conclude with a summary of our results in Section VI.

II. INTERACTIONS

In its simplest version, the scotogenic model extends the minimal SM with the addition of only a scalar doublet, η, and three neutral singlet fermions, N_k, all of which are odd under an exactly conserved Z_2 symmetry [4]. The SM particles are all even under this symmetry. Accordingly, the

lightest one of the new particles is stable and can act as DM. In this study, we consider the case that N_1 is a good candidate for cold DM [5].[1]

The Lagrangian for the interactions of the scalar particles in this model with each other and the standard $SU(2)_L \times U(1)_Y$ gauge bosons, $\boldsymbol{W}_\rho$ and B_ρ, has the form

$$\mathcal{L} = (\mathcal{D}^\rho \Phi)^\dagger \mathcal{D}_\rho \Phi + (\mathcal{D}^\rho \eta)^\dagger \mathcal{D}_\rho \eta - \mathcal{V} , \tag{1}$$

where $\mathcal{D}_\rho = \partial_\rho + (i/2)g\,\boldsymbol{\tau}{\cdot}\boldsymbol{W}_\rho + ig_Y \mathcal{Q}_Y B_\rho$,

$$\begin{aligned}
\mathcal{V} &= \mu_1^2\,\Phi^\dagger\Phi + \mu_2^2\,\eta^\dagger\eta + \tfrac{1}{2}\lambda_1(\Phi^\dagger\Phi)^2 + \tfrac{1}{2}\lambda_2(\eta^\dagger\eta)^2 \\
&\quad + \lambda_3(\Phi^\dagger\Phi)(\eta^\dagger\eta) + \lambda_4(\Phi^\dagger\eta)(\eta^\dagger\Phi) + \tfrac{1}{2}\lambda_5\big[(\Phi^\dagger\eta)^2 + (\eta^\dagger\Phi)^2\big] ,
\end{aligned} \tag{2}$$

and, after electroweak symmetry breaking,

$$\Phi = \begin{pmatrix} 0 \\ \frac{1}{\sqrt{2}}(h+v) \end{pmatrix}, \qquad \eta = \begin{pmatrix} H^+ \\ \frac{1}{\sqrt{2}}(\mathcal{S}+i\mathcal{P}) \end{pmatrix}, \tag{3}$$

with g (g_Y) being the usual $SU(2)_L$ $\big(U(1)_Y\big)$ gauge coupling constant, $\boldsymbol{\tau} = (\tau_1, \tau_2, \tau_3)$ the Pauli matrices, $\mathcal{Q}_Y$ the hypercharge operator, and v the vacuum expectation value (VEV) of Φ. The VEV of η is zero due to the Z_2 symmetry. The masses of $\mathcal{S}$, $\mathcal{P}$, and $H^\pm$ are then, respectively,

$$\begin{aligned}
m_\mathcal{S}^2 &= \mu_2^2 + \tfrac{1}{2}(\lambda_3 + \lambda_4 + \lambda_5)v^2 , \qquad m_\mathcal{P}^2 = \mu_2^2 + \tfrac{1}{2}(\lambda_3 + \lambda_4 - \lambda_5)v^2 , \\
m_H^2 &= \mu_2^2 + \tfrac{1}{2}\lambda_3\, v^2 .
\end{aligned} \tag{4}$$

In our numerical analysis in Sections IV and V, we will make the usual assumption [5] that λ_5 is very small, $|\lambda_5| \ll |\lambda_3 + \lambda_4|$, which implies that $|m_\mathcal{S}^2 - m_\mathcal{P}^2| = |\lambda_5|v^2 \ll m_\mathcal{S}^2 \simeq m_\mathcal{P}^2$. From Eq. (1), the couplings of η to h, the photon A, and the Z boson are described by

$$\begin{aligned}
\mathcal{L} \supset{}& \big[\big(\mu_2^2 - m_\mathcal{S}^2\big)\mathcal{S}^2 + \big(\mu_2^2 - m_\mathcal{P}^2\big)\mathcal{P}^2 + 2\big(\mu_2^2 - m_H^2\big)H^+ H^-\big]\frac{h}{v} \\
&+ ie\big(H^+ \partial^\rho H^- - H^- \partial^\rho H^+\big)A_\rho + e^2\,H^+ H^- A^2 + \frac{eg\big(1 - 2s_w^2\big)}{c_w} H^+ H^- A^\rho Z_\rho \\
&+ \frac{g}{2c_w}\big[\mathcal{P}\,\partial^\rho\mathcal{S} - \mathcal{S}\,\partial^\rho\mathcal{P} + i\big(1 - 2s_w^2\big)\big(H^+ \partial^\rho H^- - H^- \partial^\rho H^+\big)\big]Z_\rho ,
\end{aligned} \tag{5}$$

where only terms relevant to our processes of interest are on display, $e = gs_w > 0$ is the electromagnetic charge, and $c_w = \sqrt{1 - s_w^2} = \cos\theta_W$ with the Weinberg angle θ_W.

The new singlet fermions N_k are permitted to have Majorana masses and interact with other particles according to

$$\mathcal{L}_N = -\tfrac{1}{2}M_k\,\overline{N_k^c}\,P_R N_k + \mathcal{Y}_{jk}\big[\bar{\ell}_j H^- - \tfrac{1}{\sqrt{2}}\bar{\nu}_j\,(\mathcal{S} - i\mathcal{P})\big]P_R N_k + \text{H.c.} , \tag{6}$$

where $j, k = 1, 2, 3$ are summed over, the superscript c refers to charge conjugation, $P_R = \tfrac{1}{2}(1+\gamma_5)$, and $\ell_{1,2,3} = e, \mu, \tau$. Hence, writing the Yukawa couplings $\mathcal{Y}_{jk} = Y_{\ell_j k}$, we have

$$\mathcal{Y} = \begin{pmatrix} Y_{e1} & Y_{e2} & Y_{e3} \\ Y_{\mu1} & Y_{\mu2} & Y_{\mu3} \\ Y_{\tau1} & Y_{\tau2} & Y_{\tau3} \end{pmatrix}. \tag{7}$$

---

[1] The possibility of N_k being warm DM has also been proposed in the literature [6].

In this model the light neutrinos get mass radiatively through one-loop diagrams involving internal $\mathcal{S}$ or $\mathcal{P}$ and N_k. The mass eigenvalues m_j of the neutrinos are given by [4]

$$\text{diag}(m_1, m_2, m_3) = \mathcal{U}^{\mathrm{T}} \mathcal{M}_\nu \mathcal{U} , \tag{8}$$

$$\mathcal{M}_\nu = \mathcal{Y} \, \text{diag}(\Lambda_1, \Lambda_2, \Lambda_3) \, \mathcal{Y}^{\mathrm{T}} , \tag{9}$$

$$\Lambda_k = \frac{\lambda_5 \, v^2}{16\pi^2 \, M_k} \mathcal{I}\left(\frac{M_k^2}{m_0^2}\right) , \qquad \mathcal{I}(x) = \frac{x}{1-x} + \frac{x^2 \ln x}{(1-x)^2} , \qquad 2m_0^2 = m_{\mathcal{S}}^2 + m_{\mathcal{P}}^2 , \tag{10}$$

where $\mathcal{U}$ is the PMNS (Pontecorvo-Maki-Nakagawa-Sakata [7]) unitary matrix and the expression for Λ_k is valid for $m_0 \simeq m_{\mathcal{S}} \simeq m_{\mathcal{P}}$.

III. MIXING AND YUKAWA MATRICES

We express the PMNS mixing matrix as a product of two matrices involving only two mixing angles, θ and ς, respectively, with the latter matrix also containing a CP-violating phase δ. Thus

$$\mathcal{U} = \begin{pmatrix} \cos\theta & \sin\theta & 0 \\ \frac{-1}{\sqrt{2}}\sin\theta & \frac{1}{\sqrt{2}}\cos\theta & \frac{1}{\sqrt{2}} \\ \frac{1}{\sqrt{2}}\sin\theta & \frac{-1}{\sqrt{2}}\cos\theta & \frac{1}{\sqrt{2}} \end{pmatrix} \begin{pmatrix} \cos\varsigma & 0 & e^{i\delta}\sin\varsigma \\ 0 & 1 & 0 \\ -e^{-i\delta}\sin\varsigma & 0 & \cos\varsigma \end{pmatrix}$$

$$= \frac{1}{\sqrt{2}} \begin{pmatrix} \sqrt{2}\,\cos\theta\,\cos\varsigma & \sqrt{2}\,\sin\theta & \sqrt{2}\,e^{i\delta}\cos\theta\,\sin\varsigma \\ -\sin\theta\,\cos\varsigma - e^{-i\delta}\sin\varsigma & \cos\theta & -e^{i\delta}\sin\theta\,\sin\varsigma + \cos\varsigma \\ \sin\theta\,\cos\varsigma - e^{-i\delta}\sin\varsigma & -\cos\theta & e^{i\delta}\sin\theta\,\sin\varsigma + \cos\varsigma \end{pmatrix} . \tag{11}$$

The form of $\mathcal{U}$ with $\sin\theta = 1/\sqrt{3}$ was discussed in Ref. [8], whereas the $\varsigma = 0$ case was treated in Ref. [9]. Both of these possibilities for $\mathcal{U}$ are no longer compatible with the most recent findings, especially that $\sin\theta_{13}$ is not negligibly small [2]. Therefore, we will instead take

$$\cos\theta \, \sin\varsigma = \sin\theta_{13} , \qquad \theta \sim \theta_{12} , \tag{12}$$

which lead numerically to elements of $\mathcal{U}$ consistent with their empirical counterparts within one sigma. For simplicity, we also fix $e^{i\delta} = 1$ in accordance with the value $\delta = \left(300^{+66}_{-138}\right)^\circ$ from the latest fit to the global data [10].

Incorporating Eq. (11) into the matrix diagonalization relation in Eq. (8), we then derive the mass eigenvalues

$$\begin{aligned} m_1 = \Big\{ & Y_{ek}^2 \, c_\theta^2 \, c_\varsigma^2 - \sqrt{2}\,Y_{ek}\big[(Y_{\mu k} - Y_{\tau k})s_\theta\,c_\varsigma + (Y_{\mu k} + Y_{\tau k})s_\varsigma\big]c_\theta\,c_\varsigma \\ & + \tfrac{1}{2}\big[(Y_{\mu k} - Y_{\tau k})s_\theta\,c_\varsigma + (Y_{\mu k} + Y_{\tau k})s_\varsigma\big]^2 \Big\}\Lambda_k , \end{aligned}$$

$$m_2 = \Big[\tfrac{1}{2}(Y_{\mu k} - Y_{\tau k})^2 c_\theta^2 + \sqrt{2}\,Y_{ek}(Y_{\mu k} - Y_{\tau k})c_\theta\,s_\theta + Y_{ek}^2\,s_\theta^2\Big]\Lambda_k ,$$

$$\begin{aligned} m_3 = \Big\{ & Y_{ek}^2 \, c_\theta^2 \, s_\varsigma^2 + \sqrt{2}\,Y_{ek}\big[(Y_{\mu k} + Y_{\tau k})c_\varsigma - (Y_{\mu k} - Y_{\tau k})s_\theta\,s_\varsigma\big]c_\theta\,s_\varsigma \\ & + \tfrac{1}{2}\big[(Y_{\mu k} + Y_{\tau k})c_\varsigma - (Y_{\mu k} - Y_{\tau k})s_\theta\,s_\varsigma\big]^2 \Big\}\Lambda_k , \end{aligned} \tag{13}$$

4

where we have implicitly summed over $k = 1, 2, 3$ and adopted the notation

$$c_\theta \;=\; \cos\theta\,, \quad s_\theta \;=\; \sin\theta\,, \quad c_\varsigma \;=\; \cos\varsigma\,, \quad s_\varsigma \;=\; \sin\varsigma\,. \tag{14}$$

As will be seen shortly, these mass formulas can be rendered much simpler using the relations among $Y_{\ell k}$ which have to fulfill the required vanishing of the off-diagonal matrix elements on the right-hand side of Eq. (8). Thus we arrive at the diagonalization conditions

$$\begin{aligned}
0 \;=\; & \Big\{ \sqrt{2}\, Y_{ek}\,(Y_{\mu k} - Y_{\tau k})\big(c_\theta^2 - s_\theta^2\big)c_\varsigma + \big[2Y_{ek}^2 - (Y_{\mu k} - Y_{\tau k})^2\big]c_\theta s_\theta\, c_\varsigma \\
& - \big(Y_{\mu k}^2 - Y_{\tau k}^2\big)c_\theta\, s_\varsigma - \sqrt{2}\, Y_{ek}\,(Y_{\mu k} + Y_{\tau k})s_\theta\, s_\varsigma \Big\}\Lambda_k\,,
\end{aligned}$$

$$\begin{aligned}
0 \;=\; & \Big\{ \sqrt{2}\, Y_{ek}\,(Y_{\mu k} - Y_{\tau k})\big(c_\theta^2 - s_\theta^2\big)s_\varsigma + \big[2Y_{ek}^2 - (Y_{\mu k} - Y_{\tau k})^2\big]c_\theta s_\theta\, s_\varsigma \\
& + \big(Y_{\mu k}^2 - Y_{\tau k}^2\big)c_\theta\, c_\varsigma + \sqrt{2}\, Y_{ek}\,(Y_{\mu k} + Y_{\tau k})s_\theta\, c_\varsigma \Big\}\Lambda_k\,,
\end{aligned}$$

$$\begin{aligned}
0 \;=\; & \Big\{ \big[\big(2Y_{ek}^2 - Y_{\mu k}^2 - Y_{\tau k}^2\big)c_\theta^2 - \sqrt{8}\, Y_{ek}\,(Y_{\mu k} - Y_{\tau k})c_\theta s_\theta - 2Y_{\mu k}Y_{\tau k}\big(1 + s_\theta^2\big)\big]c_\varsigma s_\varsigma \\
& + \big[\sqrt{2}\, Y_{ek}\, c_\theta - (Y_{\mu k} - Y_{\tau k})s_\theta\big](Y_{\mu k} + Y_{\tau k})\big(c_\varsigma^2 - s_\varsigma^2\big) \Big\}\Lambda_k\,, \tag{15}
\end{aligned}$$

summation over $k = 1, 2, 3$ being again implied. It turns out that these equations are exactly solvable for Y_{ek} and $Y_{\mu k}$ in terms of $Y_k \equiv Y_{\tau k}$. As sketched in Appendix A, there are twenty-seven possible sets of solutions to Eq. (15), but three of the sets can each produce only one nonzero mass out of $m_{1,2,3}$ in Eq. (13), whereas another eighteen (six) of the sets can each lead to two (three) nonzero masses.

It is worth pointing out that the form of Eq. (9) also appears in some other models of radiative neutrino mass, which may be generated by one-loop [11] or two-loop [12] diagrams. Hence these solutions for $Y_{\ell k}$ plus the resulting masses $m_{1,2,3}$ are also applicable to such models, with $\Lambda_{1,2,3}$ encoding the model specifics.

The solutions in one of the eighteen sets that can each yield two nonzero masses are

$$\begin{aligned}
Y_{ei} \;=\; & \frac{\sqrt{2}\, c_\theta\, s_\varsigma\, Y_i}{s_\theta\, s_\varsigma + c_\varsigma}\,, \quad i = 1, 2\,, \quad Y_{e3} \;=\; \frac{-\sqrt{2}\, s_\theta\, Y_3}{c_\theta}\,, \\
Y_{\mu i} \;=\; & \frac{c_\varsigma - s_\theta\, s_\varsigma}{s_\theta\, s_\varsigma + c_\varsigma}\, Y_i\,, \qquad\qquad\quad Y_{\mu 3} \;=\; -Y_3\,. \tag{16}
\end{aligned}$$

These lead to the masses

$$m_1 \;=\; 0\,, \quad m_2 \;=\; \frac{2\Lambda_3 Y_3^2}{c_\theta^2}\,, \quad m_3 \;=\; \frac{2\big(\Lambda_1 Y_1^2 + \Lambda_2 Y_2^2\big)}{\big(s_\theta\, s_\varsigma + c_\varsigma\big)^2}\,. \tag{17}$$

Setting $\varsigma = 0$ in the last two equations, one recovers the corresponding expressions derived in Ref. [9]. Since it is now known experimentally that $\sin^2\theta_{13} = 0.0227^{+0.0023}_{-0.0024}$ [10], which is not very small, the $\varsigma = 0$ limit is no longer a good approximation. Particularly, as shown below, this nonzero θ_{13} corresponds to $Y_{ei} \simeq 0.24\, Y_{\mu i}$ and $Y_{\mu i} \simeq 0.82\, Y_{\tau i}$ in Eq. (16), compared to $Y_{ei} = 0$ and $Y_{\mu i} = Y_{\tau i}$ in the $\varsigma = 0$ case [9].

Hereafter, we will employ nonzero ς according to Eq. (12) and focus on one of the solution sets as an example that gives three nonzero masses. The solutions in this set are

$$Y_{e1} = \frac{\sqrt{2}\, c_\theta\, c_\varsigma\, Y_1}{s_\theta\, c_\varsigma - s_\varsigma}\,, \qquad Y_{e2} = \frac{-\sqrt{2}\, s_\theta\, Y_2}{c_\theta}\,, \qquad Y_{e3} = \frac{\sqrt{2}\, c_\theta\, s_\varsigma\, Y_3}{s_\theta\, s_\varsigma + c_\varsigma}\,,$$
$$Y_{\mu 1} = \frac{s_\varsigma + s_\theta\, c_\varsigma}{s_\varsigma - s_\theta\, c_\varsigma}\, Y_1\,, \qquad Y_{\mu 2} = -Y_2\,, \qquad Y_{\mu 3} = \frac{c_\varsigma - s_\theta\, s_\varsigma}{s_\theta\, s_\varsigma + c_\varsigma}\, Y_3\,, \tag{18}$$

which yield

$$m_1 = \frac{2\Lambda_1\, Y_1^2}{\left(s_\varsigma - s_\theta\, c_\varsigma\right)^2}\,, \qquad m_2 = \frac{2\Lambda_2\, Y_2^2}{c_\theta^2}\,, \qquad m_3 = \frac{2\Lambda_3\, Y_3^2}{\left(c_\varsigma + s_\theta\, s_\varsigma\right)^2}\,. \tag{19}$$

These expressions for $m_{1,2,3}$ would permit cancellations among the terms in $\Delta m_{ji}^2 = m_j^2 - m_i^2$ with larger Y_k than would the masses in Eq. (17).

Numerically, we adopt for definiteness

$$\cos\theta\, \sin\varsigma = \sqrt{0.0227}\,, \qquad \theta = 32.89°\,, \tag{20}$$

which translate into elements of $\mathcal{U}$ that are well within the one-sigma ranges of their experimental values. These choices imply the numbers collected in Table I for the Yukawa couplings and neutrino masses given in the previous two paragraphs in terms of Y_k and $\Lambda_k Y_k^2$. After applying Eqs. (18) and (19) to the constraints to be discussed in the following section, we will employ the allowed parameter values to explore several decay modes of the Higgs boson h.

TABLE I: Numerical values of $\hat{Y}_{\ell k} = Y_{\ell k}/Y_k$ and neutrino masses in terms of $\tilde{\Lambda}_k = \Lambda_k Y_k^2$ from the formulas in Eqs. (16)-(19), with the input parameters in Eq. (20).

Equations	$\hat{Y}_{e1}$	$\hat{Y}_{\mu 1}$	$\hat{Y}_{e2}$	$\hat{Y}_{\mu 2}$	$\hat{Y}_{e3}$	$\hat{Y}_{\mu 3}$	m_1	m_2	m_3
(16), (17)	0.197	0.820	0.197	0.820	-0.915	-1	0	$2.84\,\tilde{\Lambda}_3$	$1.71\big(\tilde{\Lambda}_1 + \tilde{\Lambda}_2\big)$
(18), (19)	3.293	-2.011	-0.915	-1	0.197	0.820	$15.89\,\tilde{\Lambda}_1$	$2.84\,\tilde{\Lambda}_2$	$1.71\,\tilde{\Lambda}_3$

IV. CONSTRAINTS

The couplings and masses of the nonstandard particles in the scotogenic model are subject to various constraints. Theoretically, there are a number of restrictions on the parameters λ_i in the potential in Eq. (2) and on the Yukawa couplings $\mathcal{Y}_{jk}$. Vacuum stability is ensured by demanding that $\lambda_{1,2} > 0$, $\lambda_3 > -\sqrt{\lambda_1\lambda_2}$, and $\lambda_3 + \lambda_4 \pm |\lambda_5| > -\sqrt{\lambda_1\lambda_2}$ [13]. The condition of perturbativity translates into $|\lambda_i| < 8\pi$ and $|\mathcal{Y}_{jk}| < \sqrt{4\pi}$ [14]. There are additional requirements from unitarity on some combinations or functions of λ_i [15, 16].

Experimentally, there are constraints on the masses of the new scalars. The data on W and Z widths and the null results of direct searches for new particles at $e^+ e^-$ colliders imply that [16–18]

$$m_H + m_{\mathcal{S},\mathcal{P}} > m_W\,, \qquad m_H \gtrsim 70\,\text{GeV}\,, \qquad m_{\mathcal{S}} + m_{\mathcal{P}} > m_Z\,, \tag{21}$$

where the last inequality is valid for $|m_{\mathcal{S}} - m_{\mathcal{P}}| < 8\,\text{GeV}$ [18], which pertains to our assumption that $m_{\mathcal{S}} \simeq m_{\mathcal{P}}$. Accordingly, in our numerical analysis later on we will consider the mass regions $50\,\text{GeV} \le m_{\mathcal{S},\mathcal{P}} \le 120\,\text{GeV}$ and $70\,\text{GeV} \le m_H \le 120\,\text{GeV}$. These choices respect the limits on the oblique parameters S and T at 90% CL (Confidence Level) [3, 19].

There are also experimental constraints on the Yukawa couplings $\mathcal{Y}_{jk}$ from several low-energy measurements and the observed DM relic abundance, which we address in the rest of this section. The latest LHC data on the Higgs boson imply extra restrictions on the model, which we will take into account in Section V.

A. Low-energy observables

Neutrino oscillation measurements determine the differences $\Delta_{ji}^2 = m_j^2 - m_i^2$. From the latest fit to the data [10]

$$\Delta_{21,\text{exp}}^2 \;=\; \left(7.50^{+0.18}_{-0.19}\right) \times 10^{-5}\,\text{eV}^2 \;, \qquad \Delta_{31,\text{exp}}^2 \;=\; \left(2.473^{+0.070}_{-0.067}\right) \times 10^{-3}\,\text{eV}^2 \;. \tag{22}$$

We have here assumed the normal ordering of the neutrino masses, which is preferred to the inverted ordering by the solutions in Eq. (18). In restricting the new couplings, we will then impose

$$31.0 \;<\; \frac{\Delta_{31}^2}{\Delta_{21}^2} \;<\; 35.0 \tag{23}$$

based on the 90% CL ranges of the numbers in Eq. (22).

For the masses, there are also constraints on the effective mass parameters $\langle m_\beta \rangle$ and $\langle m_{\beta\beta} \rangle$ from beta decay and neutrinoless double-beta decay experiments, respectively, and on the sum of masses, $\Sigma_k m_k$, from astrophysical and cosmological observations. The limits are [20]

$$\langle m_\beta \rangle \;=\; \sqrt{\sum_k |\mathcal{U}_{1k}|^2 m_k^2} \;<\; 2.1\,\text{eV} \;, \qquad \langle m_{\beta\beta} \rangle \;=\; \left| \sum_k \mathcal{U}_{1k}^2 m_k \right| \;<\; 0.25\,\text{eV} \;, \tag{24}$$

and $\Sigma_k m_k < (0.5\text{-}1.5)\,\text{eV}$. As it will turn out, these are less restrictive on the Yukawa couplings than the other constraints described in this subsection.

The interactions of $H^\pm$ and N_k with charged leptons give rise to the flavor-changing radiative decay $\ell_j \to \ell_i \gamma$ at one-loop order. Such decays have been searched for, with negative results so far, including the fresh one for $\mu \to e\gamma$ reported by the MEG Collaboration [21]. The experimental bounds on their branching ratios are [3, 21]

$$\mathcal{B}(\mu \to e\gamma)_{\text{exp}} \;<\; 5.7 \times 10^{-13} \;, \qquad \mathcal{B}(\tau \to e\gamma)_{\text{exp}} \;<\; 3.3 \times 10^{-8} \;,$$
$$\mathcal{B}(\tau \to \mu\gamma)_{\text{exp}} \;<\; 4.4 \times 10^{-8} \tag{25}$$

at 90% CL. Hence they put a cap on the prediction [5, 22]

$$\mathcal{B}(\ell_j \to \ell_i \gamma) \;=\; \frac{3\alpha\,\mathcal{B}(\ell_j \to \ell_i \nu\bar{\nu})}{64\pi\,G_{\text{F}}^2\,m_H^4} \left| \sum_k \mathcal{Y}_{ik}\mathcal{Y}_{jk}^* \mathcal{F}\left(M_k^2/m_H^2\right) \right|^2 \;, \tag{26}$$

where $G_{\rm F} = v^{-2}/\sqrt{2}$ is the Fermi constant,

$$\alpha \;=\; \frac{e^2}{4\pi}\,, \qquad \mathcal{F}(x) \;=\; \frac{1 - 6x + 3x^2 + 2x^3 - 6x^2\ln x}{6(1-x)^4}\,, \tag{27}$$

and numerically for $\mathcal{B}(\ell_j \to \ell_i\nu\bar\nu)$ we will use the central values of their data: $\mathcal{B}(\mu \to e\nu\bar\nu)_{\rm exp} \simeq 1$, $\mathcal{B}(\tau \to e\nu\bar\nu)_{\rm exp} = 0.1783 \pm 0.0004$, and $\mathcal{B}(\tau \to \mu\nu\bar\nu)_{\rm exp} = 0.1741 \pm 0.0004$ [3].

At one-loop level, the presence of $H^\pm$ and N_j also induces a modification to the anomalous magnetic moment a_{ℓ_i} of lepton ℓ_i given by [22]

$$\Delta a_{\ell_i} \;=\; \frac{-m_{\ell_i}^2}{16\pi^2 m_H^2} \sum_k |\mathcal{Y}_{ik}|^2\, \mathcal{F}\big(M_k^2/m_H^2\big)\,. \tag{28}$$

The existing data on $a_{e,\mu,\tau}$ and the charged-lepton masses imply that only a_μ can be significantly restrictive on the potential scotogenic effects at present. Its most up-to-date SM and experimental values differ by nearly three sigmas, $a_\mu^{\rm exp} - a_\mu^{\rm SM} = (249 \pm 87)\times 10^{-11}$ [23]. Accordingly, in view of the negative sign in Eq. (28), we may require

$$\big|\Delta a_\mu\big| \;<\; 9\times 10^{-10}\,. \tag{29}$$

This will turn out to be complementary to Eqs. (23) and (25) in restraining the Yukawa parameters.

B. Fermionic dark matter

Since we have picked N_1 to be the lightest of the nonstandard particles and serve as cold DM, it needs to account for the observed cosmic relic abundance, which therefore imposes bounds on $\mathcal{Y}_{k1}$. The N_1 annihilation cross-section $\sigma_{\rm ann}$ is related to its relic density Ω by [5, 24]

$$\Omega\hat h^2 \;=\; \frac{1.07\times 10^9\, x_f\,{\rm GeV}^{-1}}{\sqrt{g_*}\, m_{\rm Pl}\big[a + 3(b - a/4)/x_f\big]}\,, \qquad x_f \;=\; \ln\frac{0.0955\,(a + 6b/x_f)M_1\,m_{\rm Pl}}{\sqrt{g_*\, x_f}} \tag{30}$$

where $\hat h$ denotes the Hubble parameter, $m_{\rm Pl} = 1.22\times 10^{19}$ GeV is the Planck mass, g_* is the number of relativistic degrees of freedom below the freeze-out temperature $T_f = M_1/x_f$, and a and b are defined by the expansion $\sigma_{\rm ann}v_{\rm rel} = a + bv_{\rm rel}^2 + \mathcal{O}\big(v_{\rm rel}^4\big)$ in terms of the relative speed $v_{\rm rel}$ of the $N_1\bar N_1$ pair in their center-of-mass frame.

The leading contributions to $\sigma_{\rm ann}$ are the tree-level processes $N_1\bar N_1 \to \ell_i^-\ell_j^+$ and $N_1\bar N_1 \to \nu_i\bar\nu_j$ via exchanges of $H^\pm$ and $(\mathcal{S},\mathcal{P})$, respectively, each of which proceeds from diagrams in the t and u channels because of the Majorana nature of the external neutral fermions. We collect the expressions for their squared amplitudes in Appendix B for $m_0 \simeq m_\mathcal{S} \simeq m_\mathcal{P}$. If all the final-lepton masses are negligible, their combined cross-section times $v_{\rm rel}$ is

$$\sigma_{\rm ann}v_{\rm rel} \;=\; \sum_{i,j=1,2,3} \frac{|\mathcal{Y}_{i1}\mathcal{Y}_{j1}|^2 M_1^2 v_{\rm rel}^2}{48\pi}\left[\frac{M_1^4 + m_H^4}{\big(M_1^2 + m_H^2\big)^4} + \frac{M_1^4 + m_0^4}{\big(M_1^2 + m_0^2\big)^4}\right] \tag{31}$$

to second order in $v_{\rm rel}$, which implies $a = 0$ and $b \neq 0$. The $m_H = m_0$ limit of this formula agrees with that found in Ref. [5]. In our numerical computation with more general masses, we employ the

8

cross section obtained from the squared amplitudes in Appendix B and do not neglect the charged lepton masses, in which case a is also nonvanishing.

Since the solutions for $\mathcal{Y}_{k1}$ derived in Section III are all proportional to Y_1, it is the only coupling relevant to the relic density of N_1. To extract $|Y_1|$ from the empirical value of Ω, one can utilize Eq. (30) once the mass parameters $m_{0,H}$ and M_1 are specified. Thus, we present in Figure 1(a) some samples of the values of $|Y_1|$ consistent with the 90% CL range of the data $\Omega \hat{h}^2 = 0.111 \pm 0.006$ [3] over $5 \text{ GeV} \leq M_1 \leq 50 \text{ GeV}$ for the solutions in Eq. (18) and various sets of $m_{0,H}$. To offer a different perspective on the allowed values, in Figure 1(b) we display $|Y_1|$ versus m_0 for several choices of M_1 and m_H. The plot of $|Y_1|$ versus m_H could be roughly inferred from Figure 1(b) by interchanging m_0 and m_H, especially for $m_\ell \ll M_1$. Evidently, the demand that N_1 be the leading candidate for cold DM over the mass regions of interest can always be met by some values of Y_1, but their ranges are fairly limited.

Direct-search experiments for DM, which look for signals of it colliding with nuclei, may lead to further restraints on Y_1, but the existing bounds are still too weak. Since N_1 can scatter off a nucleon mainly via its one-loop Z-mediated axial-vector interactions with quarks [9, 25], the process is characterized by a spin-dependent cross-section that is relatively suppressed and in our case does not reach 10^{-41} cm^2. This is more than an order of magnitude below the strictest limit to date, measured by the XENON100 Collaboration [26].
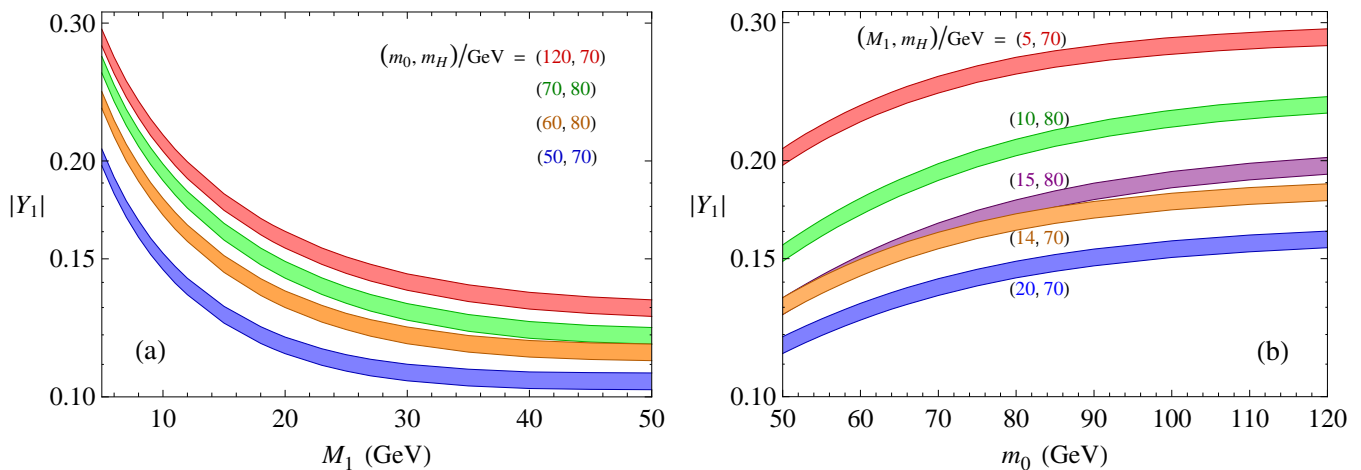
FIG. 1: Magnitude of Y_1 belonging to Yukawa couplings in Eq. (18) versus (a) M_1 and (b) m_0 satisfying the relic density constraint $0.101 \leq \Omega \hat{h}^2 \leq 0.121$ for some choices of (m_0, m_H) and (M_1, m_H), respectively.

V. IMPLICATIONS FOR HIGGS BOSON DECAY

As experimental work on the Higgs boson proceeds at the LHC with increasing precision, the accumulated data will reveal how much the properties of the particle may deviate from SM expectations. The information gained will then serve to test in particular various scenarios in which new physics can induce nonstandard decay modes of the Higgs and/or significant modifications to its SM decay channels [27]. In the scotogenic model, such effects can arise at tree and loop levels, to which we now turn. Using the parameter space allowed by the constraints discussed above, we first

look at Higgs decays into final states containing the new particles. As mentioned earlier, in our numerical work below we assume $50\,\text{GeV} \le m_0 \le 120\,\text{GeV}$ and $70\,\text{GeV} \le m_H \le 120\,\text{GeV}$.

Since collider data imply $2m_0 > m_Z$, our mass ranges of interest include $m_Z < 2m_0 \le m_h$, in which case the decay channels $h \to \mathcal{SS}, \mathcal{PP}$ are open and may be important [17]. From Eq. (5), we obtain the amplitudes for these modes at tree level to be

$$\mathcal{M}_{h\to\mathcal{SS}} \simeq \mathcal{M}_{h\to\mathcal{PP}} \simeq \frac{2\big(m_0^2 - \mu_2^2\big)}{v} \,. \tag{32}$$

Their combined rate is

$$\Gamma(h \to \eta^0\eta^0) = \Gamma(h \to \mathcal{SS}) + \Gamma(h \to \mathcal{PP}) \simeq \frac{\big(m_0^2 - \mu_2^2\big)^2}{4\pi\, m_h v^2}\sqrt{1 - \frac{4m_0^2}{m_h^2}} \,. \tag{33}$$

The decay products would be invisible for $\mathcal{S}$ and $\mathcal{P}$ lighter than N_k. Otherwise, $\mathcal{S}$ and $\mathcal{P}$ will decay into $\nu_j N_k$ and, if kinematically possible, N_k will subsequently decay into $\ell_j^+\ell_{j'}^- N_{k'}$ $\big(\bar\nu_j\nu_{j'}N_{k'}\big)$ through $H^\pm$ $(\mathcal{S},\mathcal{P})$ exchange.

In the mass range $m_h/2 < m_0 < m_h$, these two-body decays no longer happen, and so the dominant modes with $\mathcal{S}$ and $\mathcal{P}$ in the final states are the three-body decays $h \to (\mathcal{S},\mathcal{P})\nu_j N_k$ if kinematically permitted. From Eqs. (5) and (6), we obtain the tree-level amplitude

$$\mathcal{M}_{h\to\mathcal{S}(\mathcal{P})\nu_j\bar{N}_k} = (-i)\frac{\sqrt{2}}{v}\frac{\big(\mu_2^2 - m_0^2\big)\,\mathcal{Y}_{jk}\,\bar\nu_j P_R N_k}{m_0^2 - \big(p_\nu + p_N\big)^2} \tag{34}$$

and an analogous expression for $h \to \mathcal{S}(\mathcal{P})\bar\nu_j N_k$. They contribute to the combined rate

$$\Gamma\big(h \to \eta^0\nu N\big) = \sum_{\hat\eta=\mathcal{S},\mathcal{P}}\ \sum_{j,k=1,2,3}\Big[\Gamma\big(h \to \hat\eta\,\nu_j\bar{N}_k\big) + \Gamma\big(h \to \hat\eta\,\bar\nu_j N_k\big)\Big] \,. \tag{35}$$

For decays with $H^\pm$ in the final states, since collider data restrain their mass to be $m_H \gtrsim 70\,\text{GeV}$, we only have the three-body modes $h \to H^+\ell_j^-\bar{N}_k$ and their charge-conjugated counterparts, provided that $m_H + m_\ell + m_N < m_h$. As in the neutral case, we find

$$\mathcal{M}_{h\to H^+\ell_j^-\bar{N}_k} = \frac{2}{v}\frac{\big(m_H^2 - \mu_2^2\big)\,\mathcal{Y}_{jk}\,\bar\ell_j P_R N_k}{m_H^2 - \big(p_\ell + p_N\big)^2} \tag{36}$$

and similarly for $h \to H^-\ell_j^+ N_k$. They lead to the rate

$$\Gamma(h \to H\ell N) = \sum_{j,k=1,2,3}\Big[\Gamma\big(h \to H^+\ell_j^-\bar{N}_k\big) + \Gamma\big(h \to H^-\ell_j^+ N_k\big)\Big] \,, \tag{37}$$

which is identical in form to Eq. (35).

After fixing Y_1 to the range fulfilling the relic density requirement as in Section IV B, we scan all the relevant parameter space of the model subject to the constraints described in Section IV A. We find that, for the allowed coupling values, these two- and three-body decay channels of the Higgs can have enlarged rates. We illustrate this in Table II for different sets of $m_{0,H}$, μ_2, and $M_{1,2,3}$, employing

TABLE II: Sample values of mass parameters $m_{0,H}$, μ_2, and $M_{1,2,3}$, all in GeV, and Yukawa constants $Y_{1,2,3}$ satisfying the constraints discussed in Section IV. The last three columns contain the resulting branching ratio $\mathcal{B}_{\mathcal{SPH}}$, in percent, of Higgs decay into final states containing $\mathcal{S}, \mathcal{P}$, or $H^{\pm}$ and ratio $\mathcal{R}_{\gamma\mathcal{V}^0}$ of $\Gamma(h \to \gamma\mathcal{V}^0)$ to its SM value for $\mathcal{V}^0 = \gamma, Z$.

m_0	m_H	μ_2	M_1	M_2	M_3	Y_1	Y_2	Y_3	$\mathcal{B}_{\mathcal{SPH}}$	$\mathcal{R}_{\gamma\gamma}$	$\mathcal{R}_{\gamma Z}$
50	70	46 (47)	9	13	63	0.155	0.372	0.632	21 (14)	0.89 (0.89)	0.95 (0.95)
60	80	54 (56)	10	15	71	0.172	0.413	0.700	26 (14)	0.91 (0.92)	0.96 (0.97)
70	70	40i (25)	14	20	80	0.155	0.378	0.677	23 (11)	0.75 (0.83)	0.88 (0.92)
70	80	111 (99)	12	17	78	0.180	0.437	0.730	24 (12)	1.15 (1.09)	1.06 (1.04)
80	80	159 (88i)	15	22	82	0.175	0.422	0.760	22 (13)	1.53 (0.68)	1.21 (0.86)
120	70	123 (111)	20	29	85	0.157	0.386	0.715	20 (12)	1.48 (1.34)	1.20 (1.14)

the Higgs mass $m_h = 125.5\,\text{GeV}$, compatible with the most recent measurements [28], and SM Higgs total width $\Gamma_h^{\text{SM}} = 4.14\,\text{MeV}$ [29]. The numbers we have selected for $m_{0,H}$, M_1, and Y_1 can be seen to correspond to some of the points inside the colored bands on one or both graphs in Figure 1. In the tenth column of this table, we list the branching ratio $\mathcal{B}_{\mathcal{SPH}} = \Gamma_{\mathcal{SPH}}/\left(\Gamma_h^{\text{SM}} + \Gamma_{\mathcal{SPH}}\right)$ involving the rate $\Gamma_{\mathcal{SPH}}$ which is the sum of $\Gamma(h \to \eta^0\eta^0)$ or $\Gamma(h \to \eta^0\nu N)$, depending on m_0, and $\Gamma(h \to H\ell N)$. The two numbers on each line in the $\mathcal{B}_{\mathcal{SPH}}$ column correspond to the two numbers on the same line in the μ_2 column, where we have included the possibility that μ_2^2 can be negative [13]. Evidently, $\mathcal{B}_{\mathcal{SPH}}$ can be readily altered by only varying μ_2, with the other parameters fixed.

The substantial values of $\mathcal{B}_{\mathcal{SPH}}$ in this table are made possible by partial cancellations in Δm_{ji}^2 between the terms proportional to $Y_{j,i}^4$ according to Eq. (19) and in the $\ell_j \to \ell_i\gamma$ rates between the different $Y_{\ell_i k}Y_{\ell_j k}$ terms with opposite signs, as Table I indicates, which allow $Y_{1,2,3}$ not to be too suppressed by the stringent constraints. Some of such cancellations would not happen with solution sets of the type in Eq. (16). We should mention, however, that the rather sizable $Y_{1,2,3}$ can result only with some degree of fine-tuning, roughly at the per-mill level. For such Y_k and the masses in Table II, we can reproduce the measured $\Delta_{21,31}^2$ with $\lambda_5 \sim 2 \times 10^{-11}$.

To make comparison with LHC results, we find that the larger (unbracketed) numbers for $\mathcal{B}_{\mathcal{SPH}}$ in Table II have begun to be probed by bounds inferred from the latest Higgs measurements. According to several analyses [30], the current data imply that the branching ratio of nonstandard decays of the Higgs into invisible or undetected final-states can be as high as 22% at 95% CL if the Higgs production mechanism is SM-like, which is the situation in the scotogenic model. These limits are not yet very strict and, as the bracketed $\mathcal{B}_{\mathcal{SPH}}$ numbers indicate, can be easily evaded by changing μ_2, which still has a wide range of viability. Therefore, the availability of other decay modes which may provide complementary constraints would be highly desirable.

The impact of the new particles in the model can also be generated through loop diagrams.[2] Of great interest are their contributions to standard decay channels of the Higgs that are already under

---

[2] The new particles can contribute to Z-boson decays into neutrinos (charged leptons) via one-loop diagrams with internal $\mathcal{S}$ or $\mathcal{P}$ ($H^{\pm}$) and N_k. At tree level, the Z boson can also decay into three-body final states containing them, similarly to the three-body Higgs decays above. We have checked that these scotogenic effects on the Z decay are not significant.

investigation at the LHC. Here we look at $h \to \gamma\gamma$ and $h \to \gamma Z$ which arise in the SM mainly from top-quark- and W-boson-loop diagrams and also receive one-loop contributions from $H^{\pm}$. These transitions are the same as those in the inert doublet model [16, 17, 31]. Based on general results in the literature [32, 33], the predicted rates of these modes are

$$\Gamma(h \to \gamma\gamma) \;=\; \frac{\alpha^2 G_{\mathrm{F}}\, m_h^3}{128\sqrt{2}\,\pi^3} \left| \frac{4}{3}\, A_{1/2}^{\gamma\gamma}(\kappa_t) + A_1^{\gamma\gamma}(\kappa_W) + \frac{m_H^2 - \mu_2^2}{m_H^2}\, A_0^{\gamma\gamma}(\kappa_H) \right|^2 , \tag{38}$$

$$\begin{aligned}
\Gamma(h \to \gamma Z) \;=\; \frac{\alpha G_{\mathrm{F}}^2\, m_W^2 \left(m_h^2 - m_Z^2 \right)^3}{64\pi^4\, m_h^3} \Bigg| &\left(\frac{2}{c_{\mathrm{w}}} - \frac{16 s_{\mathrm{w}}^2}{3 c_{\mathrm{w}}} \right) A_{1/2}^{\gamma Z}(\kappa_t, \lambda_t) + c_{\mathrm{w}}\, A_1^{\gamma Z}(\kappa_W, \lambda_W) \\
&- \frac{\left(1 - 2 s_{\mathrm{w}}^2\right)\left(m_H^2 - \mu_2^2\right)}{c_{\mathrm{w}}\, m_H^2}\, A_0^{\gamma Z}(\kappa_H, \lambda_H) \Bigg|^2 ,
\end{aligned} \tag{39}$$

where the expressions for the form factors $A_{1/2,1,0}^{\gamma\gamma,\gamma Z}$ are available from Ref. [33], the $A_0^{\gamma\gamma,\gamma Z}$ terms originate exclusively from the $H^{\pm}$ contributions, $\kappa_X = 4 m_X^2 / m_h^2$, and $\lambda_X = 4 m_X^2 / m_Z^2$. It is worth noting that in the $m_Z = 0$ limit the amplitude for $h \to \gamma Z$ would reduce to that for $h \to \gamma\gamma$ modulo the different γ and Z couplings to fermions, W bosons, and $H^{\pm}$.

In Table II we have also listed the resulting numbers for the ratio

$$\mathcal{R}_{\gamma\mathcal{V}^0} \;=\; \frac{\Gamma(h \to \gamma\mathcal{V}^0)}{\Gamma(h \to \gamma\mathcal{V}^0)_{\mathrm{SM}}} , \qquad \mathcal{V}^0 \;=\; \gamma, Z , \tag{40}$$

where $\Gamma(h \to \gamma\mathcal{V}^0)_{\mathrm{SM}}$ is the SM rate, without the $A_0^{\gamma\mathcal{V}^0}$ part. The examples in this table demonstrate that the scotogenic effects on $\Gamma(h \to \gamma\gamma)$ and $\Gamma(h \to \gamma Z)$ have a positive correlation. Comparing the $\mathcal{B}_{\mathcal{SPH}}$ and $\mathcal{R}_{\gamma\gamma,\gamma Z}$ numbers, we see that the latter have the milder dependence on μ_2, unless μ_2^2 changes signs. Moreover, there does not appear to be a clear correlation between $\mathcal{B}_{\mathcal{SPH}}$ and the impact of $H^{\pm}$ on $\Gamma(h \to \gamma\mathcal{V}^0)$, which is partly due to the fact that the Yukawa parameters Y_k which are present in $\Gamma_{\mathcal{SPH}}$ do not contribute to $\Gamma(h \to \gamma\mathcal{V}^0)$. Since $h \to \gamma\gamma$ has been detected, unlike the γZ mode [34], we can already compare our examples with the data. The latest measurement of the signal strength for $h \to \gamma\gamma$ performed by the ATLAS Collaboration is $\sigma/\sigma_{\mathrm{sm}} = 1.6 \pm 0.3$ [35]. On the other hand, for the same mode the CMS Collaboration has found $\sigma/\sigma_{\mathrm{SM}} = 0.78 \pm 0.27$ and 1.11 ± 0.31 using two different methods [36]. While awaiting an experimental consensus on this decay channel, we can say that all of the $\mathcal{R}_{\gamma\gamma}$ numbers in Table II are still compatible with one or more of these LHC results, but the situation will likely change when more data become available. We may also expect that supplementary information will be supplied by future observations of $h \to \gamma Z$.

We have seen that there are some decay modes of the Higgs boson that can be employed to test the scotogenic model in complementary ways. At this point the restrictions inferred from the existing data on the Higgs decays are not yet strong, but already start to probe the parameter space allowed by other data. In addition, with the fairly large Yukawa couplings which we have obtained and the relatively light charged scalars, direct searches at the LHC may offer extra tests [37] on the scenario treated here.

VI. CONCLUSIONS

We have explored for the scotogenic model of radiative neutrino mass some implications of the recent discovery of a Higgs boson at the LHC and experimental determination of $\sin\theta_{13}$ that is not very small. Employing a two-parameter neutrino-mixing matrix which is consistent with the latest neutrino-oscillation data within one sigma, we derive solutions for the Yukawa couplings of the nonstandard particles in the model, which consist of scalars and fermions. Such solutions are also applicable to some other models of radiative neutrino mass. We select one of the new fermions to be the lightest of the nonstandard particles which plays the role of cold DM. Subsequently, taking into account various constraints, including those from low-energy measurements and the observed relic density, we use the solutions for the Yukawa couplings to consider Higgs decays into final states containing the new particles. We find that within the allowed parameter regions the rates of such decays can be significant, which can already be probed with the latest Higgs measurements. We also examine how these exotic decay channels may correlate with the scotogenic effects on the Higgs decays into $\gamma\gamma$ and γZ, which are under intensive study at the LHC. Consequently, upcoming Higgs data with improved precision from the LHC, or a future Higgs factory, can be expected to reveal hints of the new particles or impose further restrictions on the model.

Appendix A: Solutions for Yukawa couplings $\mathcal{Y}_{jk}$

One can solve the diagonalization conditions in Eq. (15) exactly for the three pairs of Yukawa couplings $(Y_{ek}, Y_{\mu k})$, $k = 1, 2, 3$, in terms of $Y_k = Y_{\tau k}$. There is more than one set of the solutions. In each set, we can express the pairs as $(Y_{ek}, Y_{\mu k}) = (\bar{e}_z, \bar{\mu}_z)Y_k$, where $z = a, b,$ or c and

$$
\bar{e}_a = \frac{\sqrt{2}\, c_\theta\, c_\varsigma}{s_\theta\, c_\varsigma - s_\varsigma}\,, \qquad \bar{e}_b = \frac{-\sqrt{2}\, s_\theta}{c_\theta}\,, \qquad \bar{e}_c = \frac{\sqrt{2}\, c_\theta\, s_\varsigma}{s_\theta\, s_\varsigma + c_\varsigma}\,,
$$
$$
\bar{\mu}_a = \frac{s_\varsigma + s_\theta\, c_\varsigma}{s_\varsigma - s_\theta\, c_\varsigma}\,, \qquad \bar{\mu}_b = -1\,, \qquad \bar{\mu}_c = \frac{c_\varsigma - s_\theta\, s_\varsigma}{s_\theta\, s_\varsigma + c_\varsigma}\,. \tag{A1}
$$

Since two or all three of the pairs may share the same z, such as in Eq. (16), there are altogether 27 sets of the solutions to Eq. (15). Not all of them can lead to at least two nonzero masses among the eigenvalues in Eq. (13). Three of the sets can each only yield one nonzero mass, whereas 18 (six) of the others can lead to two (three) nonzero masses.

Appendix B: Dark matter annihilation amplitudes

The Majorana nature of N_j implies that the process $N_k \bar{N}_l \to \ell_i^- \ell_j^+$ arises from H-mediated t- and u-channel diagrams. We find the absolute square of its amplitude, averaged (summed) over

initial (final) spins, to be

$$\overline{\left|\mathcal{M}_{N_k \bar{N}_l \to \ell_i^- \ell_j^+}\right|^2} = |\mathcal{Y}_{ik}\,\mathcal{Y}_{jl}|^2 \frac{\left(M_k^2 + m_{\ell_i}^2 - t\right)\left(M_l^2 + m_{\ell_j}^2 - t\right)}{4\left(m_H^2 - t\right)^2}$$
$$+ |\mathcal{Y}_{il}\,\mathcal{Y}_{jk}|^2 \frac{\left(M_k^2 + m_{\ell_j}^2 - u\right)\left(M_l^2 + m_{\ell_i}^2 - u\right)}{4\left(m_H^2 - u\right)^2}$$
$$+ \operatorname{Re}\!\left(\mathcal{Y}_{ik}^*\,\mathcal{Y}_{jl}\,\mathcal{Y}_{il}\,\mathcal{Y}_{jk}^*\right) \frac{M_k M_l \left(m_{\ell_i}^2 + m_{\ell_j}^2 - s\right)}{2\left(m_H^2 - t\right)\left(m_H^2 - u\right)} , \tag{B1}$$

where

$$s = \left(p_{N_k} + p_{N_l}\right)^2 , \qquad t = \left(p_{N_k} - p_{\ell_i}\right)^2 , \qquad u = \left(p_{N_k} - p_{\ell_j}\right)^2 . \tag{B2}$$

In the case of $N_k \bar{N}_l \to \nu_i \bar{\nu}_j$, proceeding from $(\mathcal{P}, \mathcal{S})$-mediated t- and u-channel diagrams, we need to take into account the Majorana nature of the final neutrinos as well. It follows that for $m_0 \simeq m_{\mathcal{S}} \simeq m_{\mathcal{P}}$ and negligible ν masses

$$\overline{\left|\mathcal{M}_{N_k \bar{N}_l \to \nu_i \bar{\nu}_j}\right|^2} = |\mathcal{Y}_{ik}\,\mathcal{Y}_{jl}|^2 \frac{\left(M_k^2 - t\right)\left(M_l^2 - t\right)}{4\left(m_0^2 - t\right)^2} + |\mathcal{Y}_{il}\,\mathcal{Y}_{jk}|^2 \frac{\left(M_k^2 - u\right)\left(M_l^2 - u\right)}{4\left(m_0^2 - u\right)^2}$$
$$- \operatorname{Re}\!\left(\mathcal{Y}_{ik}^*\,\mathcal{Y}_{jl}\,\mathcal{Y}_{il}\,\mathcal{Y}_{jk}^*\right) \frac{M_k M_l \, s}{2\left(m_0^2 - t\right)\left(m_0^2 - u\right)} , \tag{B3}$$

where now $t = \left(p_{N_k} - p_{\nu_i}\right)^2$ and $u = \left(p_{N_k} - p_{\nu_j}\right)^2$.

[1] G. Aad *et al.* [ATLAS Collaboration], Phys. Lett. B **716**, 1 (2012) [arXiv:1207.7214 [hep-ex]]; S. Chatrchyan *et al.* [CMS Collaboration], Phys. Lett. B **716**, 30 (2012) [arXiv:1207.7235 [hep-ex]]; http://press.web.cern.ch/press-releases/2013/03/new-results-indicate-particle-discovered-cern-higgs-boson.

[2] F.P. An *et al.* [DAYA-BAY Collaboration], Phys. Rev. Lett. **108**, 171803 (2012) [arXiv:1203.1669 [hep-ex]]; J.K. Ahn *et al.* [RENO Collaboration], Phys. Rev. Lett. **108**, 191802 (2012) [arXiv:1204.0626 [hep-ex]].

[3] J. Beringer *et al.* [Particle Data Group Collaboration], Phys. Rev. D **86**, 010001 (2012).

[4] E. Ma, Phys. Rev. D **73**, 077301 (2006) [hep-ph/0601225].

[5] J. Kubo, E. Ma, and D. Suematsu, Phys. Lett. B **642**, 18 (2006) [hep-ph/0604114].

[6] D. Aristizabal Sierra, J. Kubo, D. Restrepo, D. Suematsu, and O. Zapata, Phys. Rev. D **79**, 013011 (2009) [arXiv:0808.3340 [hep-ph]]; G.B. Gelmini, E. Osoba, and S. Palomares-Ruiz, Phys. Rev. D **81**, 063529 (2010) [arXiv:0912.2478 [hep-ph]]; E. Ma, Phys. Lett. B **717**, 235 (2012) [arXiv:1206.1812 [hep-ph]]; P.K. Hu, arXiv:1208.2613 [hep-ph].

[7] Z. Maki, M. Nakagawa, and S. Sakata, Prog. Theor. Phys. **28**, 870 (1962); B. Pontecorvo, Sov. Phys. JETP **26** (1968) 984 [Zh. Eksp. Teor. Fiz. **53** (1968) 1717].

[8] X.G. He and A. Zee, Phys. Rev. D **84**, 053004 (2011) [arXiv:1106.4359 [hep-ph]].

[9] D. Suematsu, T. Toma, and T. Yoshida, Phys. Rev. D **79**, 093004 (2009) [arXiv:0903.0287 [hep-ph]].

[10] M.C. Gonzalez-Garcia, M. Maltoni, J. Salvado, and T. Schwetz, JHEP **1212**, 123 (2012) [arXiv:1209.3023 [hep-ph]].

[11] Y. Cai, X.G. He, M. Ramsey-Musolf, and L.H. Tsai, JHEP **1112**, 054 (2011) [arXiv:1108.0969 [hep-ph]]; K. Kumericki, I. Picek, and B. Radovcic, JHEP **1207**, 039 (2012) [arXiv:1204.6597 [hep-ph]]; Phys. Rev. D **86**, 013006 (2012) [arXiv:1204.6599 [hep-ph]].

[12] G. Guo, X.G. He, and G.N. Li, JHEP **1210**, 044 (2012) [arXiv:1207.6308 [hep-ph]]; G.N. Li, G. Guo, B. Ren, Y.J. Zheng, and X.G. He, JHEP **1304**, 026 (2013) [arXiv:1212.5528 [hep-ph]].

[13] N.G. Deshpande and E. Ma, Phys. Rev. D **18**, 2574 (1978).

[14] S. Kanemura, T. Kasai, and Y. Okada, Phys. Lett. B **471**, 182 (1999) [hep-ph/9903289].

[15] S. Kanemura, T. Kubota, and E. Takasugi, Phys. Lett. B **313**, 155 (1993) [hep-ph/9303263]; A.G. Akeroyd, A. Arhrib, and E.M. Naimi, Phys. Lett. B **490**, 119 (2000) [hep-ph/0006035].

[16] A. Arhrib, R. Benbrik, and N. Gaur, Phys. Rev. D **85**, 095021 (2012) [arXiv:1201.2644 [hep-ph]].

[17] Q.H. Cao, E. Ma, and G. Rajasekaran, Phys. Rev. D **76**, 095011 (2007) [arXiv:0708.2939 [hep-ph]].

[18] A. Pierce and J. Thaler, JHEP **0708**, 026 (2007) [hep-ph/0703056 [HEP-PH]]; E.M. Dolle and S. Su, Phys. Rev. D **80**, 055012 (2009) [arXiv:0906.1609 [hep-ph]].

[19] R. Barbieri, L.J. Hall, and V.S. Rychkov, Phys. Rev. D **74**, 015007 (2006) [hep-ph/0603188].

[20] C. Kraus *et al.*, Eur. Phys. J. C **40**, 447 (2005) [hep-ex/0412056]; V.N. Aseev *et al.* [Troitsk Collaboration], Phys. Rev. D **84**, 112003 (2011) [arXiv:1108.5034 [hep-ex]]; W. Rodejohann, J. Phys. G **39**, 124008 (2012) [arXiv:1206.2560 [hep-ph]]; A. Gando *et al.* [KamLAND-Zen Collaboration], Phys. Rev. Lett. **110**, 062502 (2013) [arXiv:1211.3863 [hep-ex]].

[21] J. Adam *et al.* [MEG Collaboration], arXiv:1303.0754 [hep-ex].

[22] E. Ma and M. Raidal, Phys. Rev. Lett. **87**, 011802 (2001) [Erratum-ibid. **87**, 159901 (2001)] [hep-ph/0102255].

[23] T. Aoyama, M. Hayakawa, T. Kinoshita, and M. Nio, Phys. Rev. Lett. **109**, 111808 (2012) [arXiv:1205.5370 [hep-ph]].

[24] G. Jungman, M. Kamionkowski, and K. Griest, Phys. Rept. **267**, 195 (1996) [hep-ph/9506380].

[25] Q.H. Cao, E. Ma, and G. Shaughnessy, Phys. Lett. B **673**, 152 (2009) [arXiv:0901.1334 [hep-ph]].

[26] E. Aprile *et al.* [XENON100 Collaboration], arXiv:1301.6620 [astro-ph.CO].

[27] Some examples are discussed in A. Pilaftsis, Z. Phys. C **55**, 275 (1992) [hep-ph/9901206]; J.L. Diaz-Cruz and J.J. Toscano, Phys. Rev. D **62**, 116005 (2000) [hep-ph/9910233]; S. Kanemura, T. Ota, and K. Tsumura, Phys. Rev. D **73**, 016006 (2006) [hep-ph/0505191]; J.H. Chen, X.G. He, J. Tandean, and L.H. Tsai, Phys. Rev. D **81**, 113004 (2010) [arXiv:1001.5215 [hep-ph]]; G. Blankenburg, J. Ellis, and G. Isidori, Phys. Lett. B **712**, 386 (2012) [arXiv:1202.5704 [hep-ph]]; L. Wang and X.F. Han, Phys. Rev. D **86**, 095007 (2012) [arXiv:1206.1673 [hep-ph]]; Phys. Rev. D **87**, 015015 (2013) [arXiv:1209.0376 [hep-ph]]; N. Bonne and G. Moreau, Phys. Lett. B **717**, 409 (2012) [arXiv:1206.3360 [hep-ph]]; P.S. Bhupal Dev, R. Franceschini, and R.N. Mohapatra, Phys. Rev. D **86**, 093010 (2012) [arXiv:1207.2756 [hep-ph]]; A. Alves, A.G. Dias, E.R. Barreto, C.A. de S.Pires, F.S. Queiroz, and P.S.R. da Silva, Eur. Phys. J. C **73**, 2288 (2013) [arXiv:1207.3699 [hep-ph]]; C.G. Cely, A. Ibarra, E. Molinaro, and S.T. Petcov, Phys. Lett. B **718**, 957 (2013) [arXiv:1208.3654 [hep-ph]]; R. Harnik, J. Kopp, and J. Zupan, JHEP **1303**, 026 (2013) [arXiv:1209.1397 [hep-ph]]; G. Moreau, Phys. Rev. D **87**, 015027 (2013) [arXiv:1210.3977 [hep-ph]]; A. Arhrib, Y. Cheng, and O.C.W. Kong, Phys. Rev. D **87**, 015025 (2013) [arXiv:1210.8241 [hep-ph]]; S. Davidson and P. Verdier, Phys. Rev. D **86**, 111701 (2012) [arXiv:1211.1248 [hep-ph]]; C.W. Chiang, T. Nomura, and J. Tandean, Phys. Rev. D **87**, 075020 (2013) [arXiv:1302.2894 [hep-ph]]; A. Dery, A. Efrati, Y. Hochberg, and Y. Nir, arXiv:1302.3229 [hep-ph].

[28] ATLAS Collaboration, Report No. ATLAS-CONF-2013-014, March 2012; CMS Collaboration, Report

No. CMS-PAS-HIG-12-045, November 2012.

[29] S. Dittmaier *et al.*, arXiv:1201.3084 [hep-ph]; https://twiki.cern.ch/twiki/bin/view/LHCPhysics/CERNYellowReportPageBR2.

[30] K. Cheung, J.S. Lee, and P.Y. Tseng, arXiv:1302.3794 [hep-ph]; A. Falkowski, F. Riva, and A. Urbano, arXiv:1303.1812 [hep-ph]; P.P. Giardino, K. Kannike, I. Masina, M. Raidal, and A. Strumia, arXiv:1303.3570 [hep-ph]; J. Ellis and T. You, arXiv:1303.3879 [hep-ph].

[31] D. Borah and J.M. Cline, Phys. Rev. D **86**, 055001 (2012) [arXiv:1204.4722 [hep-ph]]; B. Swiezewska and M. Krawczyk, arXiv:1212.4100 [hep-ph]; A. Goudelis, B. Herrmann, and O. Stal, arXiv:1303.3010 [hep-ph].

[32] A. Djouadi, Phys. Rept. **457**, 1 (2008) [hep-ph/0503172]; Phys. Rept. **459**, 1 (2008) [hep-ph/0503173]; M. Carena, I. Low, and C.E. M. Wagner, JHEP **1208**, 060 (2012) [arXiv:1206.1082 [hep-ph]]; W.F. Chang, J.N. Ng, and J.M.S. Wu, Phys. Rev. D **86**, 033003 (2012) [arXiv:1206.5047 [hep-ph]]; C.W. Chiang and K. Yagyu, Phys. Rev. D **87**, 033003 (2013) [arXiv:1207.1065 [hep-ph]]; references therein.

[33] C.S. Chen, C.Q. Geng, D. Huang, and L.H. Tsai, Phys. Rev. D **87**, 075019 (2013) [arXiv:1301.4694 [hep-ph]].

[34] ATLAS Collaboration, Report No. ATLAS-CONF-2013-009, March 2013; CMS Collaboration, Report No. CMS-PAS-HIG-13-006, March 2013.

[35] ATLAS Collaboration, Report No. ATLAS-CONF-2013-014, March 2013.

[36] CMS Collaboration, Report No. CMS-PAS-HIG-13-001, March 2013.

[37] S. Bhattacharya, E. Ma, A. Natale, and A. Rashed, arXiv:1302.6266 [hep-ph].